Effect of Channel Impairments on the Performance of Burst-Mode Receivers in Gigabit PON

Bhavin J. Shastri, Noha Kheder, and David V. Plant
Photonic Systems Group, Department of Electrical and Computer Engineering, McGill University, Montréal, QC H3A 2A7, Canada
shastri@ieee.org

***Abstract*—We experimentally study the effect of channel impairments on the performance of a burst-mode receiver (BMRx) in a 622 Mb/s 20-km gigabit-capable passive optical network (GPON) uplink. Specifically, we study the impact of mode-partition noise in the GPON uplink in terms of the bit-error rate (BER) and the packet loss ratio (PLR) performance of the system. Our receiver features automatic phase acquisition using a clock phase aligner (CPA), and forward-error correction using $(255, 239)$ Reed-Solomon codes. The BMRx provides instantaneous (0 preamble bit) phase acquisition and a PLR $< 10^{-6}$ for any phase step ($\pm 2\pi$ rads) between consecutive packets. The receiver also accomplishes a 3 dB coding gain at a BER $= 10^{-10}$. The CPA makes use of a phase picking algorithm and an oversampling clock and data recovery circuit operated at twice the bit rate.**

I. Introduction

Passive optical networks (PONs) are an emerging multi-access network technology based on all-optical core. PONs are expected to solve the so called "last mile problem", that remains a bottleneck between the backbone network and high-speed local area networks [1]. PONs provide a low-cost solution, with a guaranteed quality of service of deploying fiber-to-the-home/premises (FTTx), which is an effective solution to enable new multimedia services [2].

Fig. 1 shows an example of a gigabit-capable PON (GPON) network. In the downstream direction, the network is point-to-point. Continuous data is broadcast from the optical line terminator (OLT) to the optical network units (ONUs) using time division multiplexing (TDM) in the 1480-1550-nm wavelength band. The transmit side of the OLT and the receive side of the ONUs can therefore use continuous mode ICs.

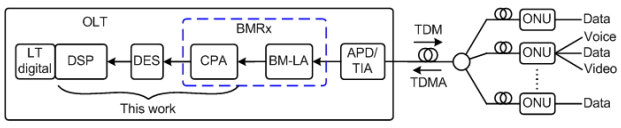

Fig. 1. Generic GPON network for FTTx showing our work in context (LT: line terminator; DSP: digital signal processing; DES: deserializer; APD: avalanche photodiode; TIA: transimpedance amplifier).

The challenge in the design of a chip set for PONs comes from the upstream data path. In the upstream direction, the network is point-to-multipoint: using time division multiple access (TDMA), multiple ONUs transmit bursty data in the 1310-nm window to the OLT in the central office. Because of optical path differences in the upstream path, packets can vary in phase and amplitude. To deal with these variations, the OLT requires a burst-mode receiver (BMRx). The BMRx is responsible for amplitude and phase recovery, which must be achieved at the beginning of every packet. At the front-end of the BMRx is a burst-mode limiting amplifier (BM-LA) responsible for amplitude recovery. Then, clock and data recovery (CDR) is performed with phase acquisition by a clock phase aligner (CPA). This paper focuses on the CPA aspect of the BMRx.

Current PON systems employ Fabry-Perot (FP) lasers, a multi-longitudinal mode device, at the ONU. FP lasers provide the most cost effective solution for meeting the PON requirements, that is, the optical power required for a 20-km reach in the 1310-1550-nm range. However, the bit-error rate (BER) and the packet loss ratio (PLR) performance of the optical system may be severely impaired by the mode-partition noise (MPN) of a FP laser coupled with the chromatic dispersion that exists in the transmission fiber [3]. Thus, MPN introduces a limitation in the length of the optical link.

In this paper, we experimentally study the impact of channel impairments on the performance of a BMRx in a 622 Mb/s 20-km GPON uplink[1]. More specifically, we study the impact of MPN in terms of the BER and the PLR performance of the system. We also extend on the results presented in [5], [6] which were based on an emulated PON electrical test-bed.

II. Experimental Setup

A block diagram of the GPON uplink experimental setup is shown in Fig. 2. A 1310-nm laser is modulated with upstream PON traffic using an electro-optic modulator (EOM). The modulated signal is then sent through 20 km of single-mode fiber (SMF-28). The desired information rate is 622 Mb/s. As the forward-error correction (FEC) Reed-Solomon (RS) $(255, 239)$ code introduces $\sim 15/14$ overhead, we used an aggregate bit rate of 666.43 Mb/s. A variable optical attenuator (VOA) serves to control the received power level. The optical to electrical conversion is performed by a photodetector. The electrical signal is then low-pass filtered (LPF) by a fourth-order Bessel-Thomson filter whose -3-dB cutoff frequency is $0.7 \times$ bit rate, or 467 MHz. Such a filter has an optimum

[1]Note, as per the ITU-T G.984.2 standard, the downstream nominal line rates can be 1.25 Gb/s or 2.5 Gb/s, while the upstream nominal line rates can be 155 Mb/s, 622 Mb/s, 1.25 Gb/s, or 2.5 Gb/s [4].

978-1-4244-2167-1/08/$25.00 ©2008 IEEE

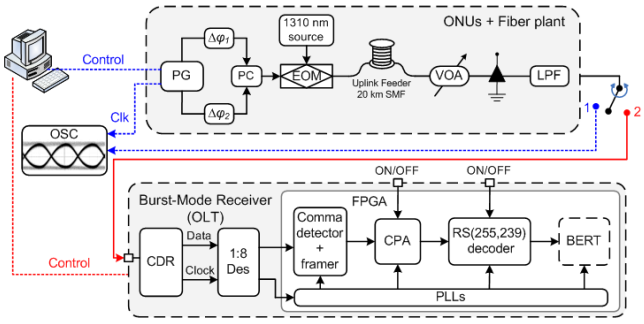

Fig. 2. Block diagram of 622 Mb/s GPON experimental setup with the BMRx (OSC: oscilloscope).

bandwidth to filter out noise while keeping inter-symbol interference to a minimum [7].

The bursty upstream PON traffic as in [6], is generated with adjustable phase ($-2\pi \leq \Delta\varphi \leq +2\pi$ rads) from programmable ports of a pattern generator (PG), which are then concatenated via a power combiner (PC) and used to drive the EOM. These packets are formed from: 16 guard bits, 0 to 28 (l) preamble bits, 20 delimiter bits, $2^{15}-1$ payload bits, and 48 comma bits. The guard, preamble, and delimiter bits correspond to the physical-layer upstream burst-mode overhead of 8 bytes at 622 Mb/s as specified by the G.984.2 standard [4]. The guard bits provide distance between two consecutive packets to avoid collisions. The preamble field is used to perform amplitude and phase recovery. The delimiter is a unique pattern indicating the start of the packet to perform byte synchronization. Likewise, the comma is a unique pattern to indicate the end of the payload. The payload is simply a nonreturn-to-zero $2^{15}-1$ pseudorandom binary sequence. The PLR and the BER are measured on the payload bits only. We define the lock acquisition time corresponding to the number of bits (l) in front of the delimiter in order to get error free operation (PLR $< 10^{-6}$ and BER $< 10^{-10}$) for any phase step $|\Delta\varphi| \leq 2\pi$ rads, between consecutive packets.

The BMRx at the OLT includes a multi-rate CDR from Analog Devices (ADN2819), a 1:8 deserializer from Maxim-IC (MAX3885), and a CPA module and a FEC RS$(255, 239)$ decoder implemented on a field programmable gate array (FPGA). The CDR recovers the clock and the data from the incoming signal. The CDR supports the following frequencies of interest: 622 Mb/s (without FEC), 666.43 Mb/s (with FEC), and 1.25 Gb/s. The latter frequency provides $2\times$ oversampling. Oversampling, together with a phase picking algorithm, provides the core of the burst-mode CDR. The CDR is followed by a 1:8 deserializer. The lower rate parallel data is then sent to the FPGA for further processing. The framer and comma detector, the CPA, phase-locked loops (PLLs), and the RS$(255, 239)$ decoder, are implemented on the FPGA alongside a BER tester (BERT). A computer is used to control the output of the pattern generator and to communicate with the FPGA on the receiver. Automatic detection of the payload is implemented on the FPGA through a framer and a comma detector that are responsible for detecting the beginning (delimiter bits) and the end (comma bits) of the packet, respectively. The CPA makes use of a phase picking algorithm in [5] with the CDR operated in $2\times$ oversampling mode. The CPA is turned on for the PLR measurements with phase acquisition for burst-mode reception when $\Delta\varphi \neq 0$ rad; otherwise it can be by-passed for continuous-mode reception when $\Delta\varphi = 0$ rad. The realigned data is then sent to the RS decoder which is turned on for the BER measurements with FEC, otherwise it is by-passed.

III. Experimental Results and Discussions

A. Bit-Error Rate Measurements

To study the impact of FEC on the optical budget of the GPON uplink, we plot the BER performance of the system with and without FEC, as a function of the received power as shown in Fig. 3(a). Note that the abscissa is the useful power, that is, the optical power contributed at the photodiode. According to the G.984.2 standard, coding gain is defined as the difference in input power at the receiver with and without FEC at a BER $= 10^{-10}$. We observe a coding gain of $\sim$3 dB.

Let us make a comparison between the experimental BER using FEC and the simulations results. Let p_e be the measured BER without FEC. Organizing the bits in symbols of m bits yields an equivalent symbol-error rate p_S, under the assumption of purely random bit errors, as

$$p_S = 1 - (1 - p_e)^m \tag{1}$$

The RS(n, k) = RS$(255, 239)$ block-based FEC code divides a codeword of n symbols into 8-bit symbols and k data (uncoded) symbols, yielding in a memoryless channel, a symbol-error rate after FEC p_s^{FEC} of [8]

$$p_S^{FEC} \approx \frac{1}{2^m - 1} \sum_{j=t+1}^{2^m-1} j \binom{2^m - 1}{j} p_S^j (1 - p_S)^{2^m - 1 - j} \tag{2}$$

where $t = \left\lfloor \frac{n-k}{2} \right\rfloor$ is the symbol-error correcting capability of the code. Again, assuming a memoryless channel and since we are using orthogonal signaling (on-off keying), the lower bound of the BER after FEC p_e^{FEC}, can be calculated as

$$p_e^{FEC} \geq \frac{p_S^{FEC}}{m} \tag{3}$$

We plot the purely random and memoryless channel prediction of the BER after FEC p_e^{FEC}, and our experimental results in Fig. 3(a). The BER performance is a function of intrinsic and extrinsic effects of the channel. That is, the presence of random and deterministic errors will affect the error correcting capability of the FEC code. It can be observed that the simulation and the experimental results are in close agreement for BER $> 10^{-4}$. This is because for lower signal power, random errors dominate over deterministic errors in the system. However, for BER $< 10^{-4}$, we observe $\sim$0.5 dB of power penalty between the simulation and the experimental results; our predictions are optimistic. Since (1) - (3), assume purely random bit errors and a memoryless channel, p_e^{FEC} is

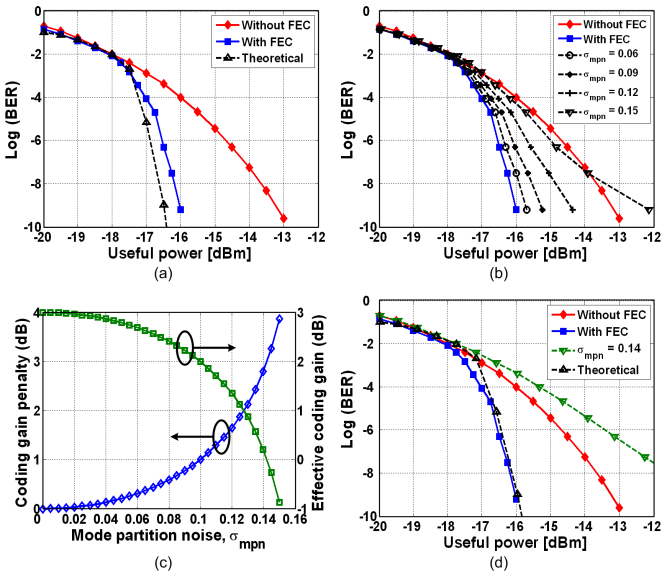

Fig. 3. (a) BER performance. (b) Effect of MPN. (c) Effective coding gain and MPN penalty. (d) Theoretical effective coding gain with worst-case MPN.

overestimated for BER $< 10^{-4}$. This is attributed to the fact that as the received power is increased, the presence of random errors is attenuated relative to the presence of deterministic errors. This is more likely due to the memory added in the channel through intensity noise, deterministic jitter, CDR, and other components, making the errors statistically dependent in a GPON uplink. An interleaver may be used to arrange the data in a non-contiguous way such that the codeword bits are interleaved before being transmitted. Thus, in the presence of deterministic jitter, only a correctable number of bits in each codeword will be affected. This however, increases latency.

MPN is a phenomenon occurring because of an anti-correlation among pairs of longitudinal modes and has been studied extensively in [9]. That is, even though the total intensity of the modes remains relatively constant, various longitudinal modes fluctuate in such a way that individual modes exhibit large intensity fluctuations [3]. This leads to the different modes becoming unsynchronized because of group-velocity dispersion. Thus, the signal-to-noise ratio (SNR) at the decision circuit becomes worse than that expected in the absence of MPN. Consequently, a power penalty must be paid to improve the SNR to the same value that is necessary to achieve the required BER. The power penalty caused by MPN existing in 1330-nm lightwave systems has been analyzed in [10].

Suppose the time average spectrum of the laser source is assumed to be Gaussian and the half spectrum width is σ_λ, then the mean square variance of MPN σ_{mpn}, is determined by [10]

$$\sigma_{mpn} = \frac{k}{\sqrt{2}}\left[1 - e^{-(\pi BDL\sigma_\lambda)^2}\right] \tag{4}$$

where k is the mode partition coefficient, B is the bit rate, D is the fiber delay dispersion per unit lengh per unit wavelength, and L is the fiber length. If MPN did not exist in the system, the signal power S_o which is required to achieve a given BER would be $1/Q^2 = (\sigma_o/S_o)^2$ where σ_o is the total receiver power and Q is determined by the BER $p_e = \frac{1}{2}\operatorname{erfc}\left(\frac{Q}{\sqrt{2}}\right)$. The required signal power S_m to achieve the same BER when MPN is added to the receiver noise becomes [11]

$$\frac{1}{Q^2} = \left(\frac{\sigma_o}{S_m}\right)^2 + \sigma_{mpn}^2 \tag{5}$$

and the resulting power penalty caused by MPN δ_{mpn}, is then [9]

$$\delta_{mpn} = 10\log\left(\frac{S_m}{S_o}\right) = -5\log\left(1 - Q^2\sigma_{mpn}^2\right) \tag{6}$$

The coding gain G (when $\sigma_{mpn} = 0$) obtained by employing FEC will then also have to compensate for the power penalty δ_{mpn}, giving an MPN power penalty after FEC δ_{mpn}^{FEC}. Consequently, the effective coding gain G_{eff} (when $\sigma_{mpn} \neq 0$) of the system will decrease with an increase in MPN, giving a limitation on how much MPN can be tolerated in the GPON uplink. It can be expressed as

$$G_{eff}|_{\sigma_{mpn}\neq 0} = G|_{\sigma_{mpn}=0} - \delta_{mpn}^{FEC} \tag{7}$$

In Fig. 3(b), we plot the BER with FEC, for various values of the mean square variance of MPN σ_{mpn}. As expected, the system performance degrades with an increase in σ_{mpn}. More specifically, from Fig. 3(c) we observe that as the σ_{mpn} in the system increases, the coding gain penalty increases exponentially, while the effective coding gain decreases very rapidly. The maximum MPN that can be tolerated in the uplink giving an effective coding gain of zero, is when $\sigma_{mpn} \sim 0.14$.

Let us assume that the GPON uplink is a memoryless channel and that the presence of deterministic errors is negligible. According to the statistical analysis of MPN presented in [9], [10], MPN penalty will lead to independent (random) errors. We can then use (1) - (3), and estimate the theoretical bound when RS$(255, 239)$ codes are employed to correct for the power penalty introduced by MPN. In Fig. 3(d) we plot the BER performance of the system with and without FEC, and also the theoretical bound obtained for the worst case MPN, when $\sigma_{mpn} = 0.14$. The effective coding gain is observed to be $\sim$3 dB. However, note that for $\sigma_{mpn} = 0.14$, we obtained an effective coding gain of zero from Fig. 3(c). This means that the 'extra' power penalty that we observed must be due to deterministic errors present in the GPON uplink.

B. Packet-Loss Ratio Measurements

PLR performance of the GPON uplink as a function of the phase step between consecutive packets is shown in Fig. 4(a). Let us first consider the case for a back-to-back configuration, that is, without the 20-km of fiber. With only the CDR, and the CPA turned off, the curve exhibits symmetry about the worst-case phase step at $\Delta\varphi = \pi$ rads $(800$ ps$)$ as the CDR is sampling on the edge of the data eye. Preamble bits ('1010 . . .' pattern) can be inserted at the beginning of the packets to help the CDR settle down and acquire lock. As the preamble length

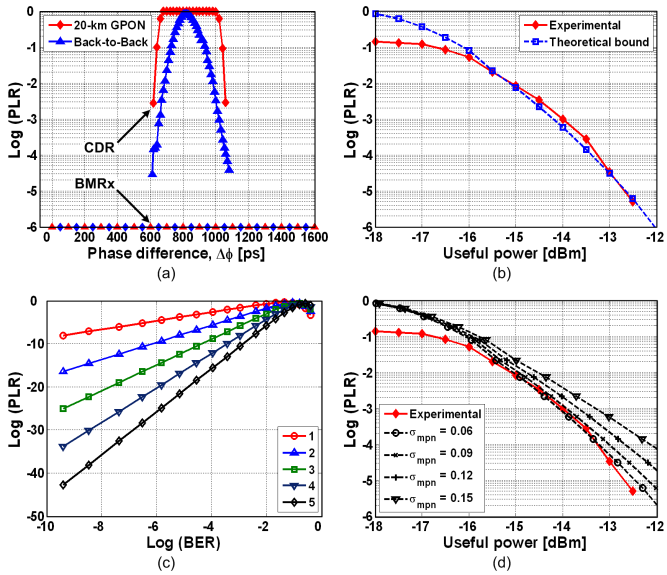

Fig. 4. (a) PLR performance. (b) Comparison of simulated and measured PLR. (b) PLR vs. BER performance with a pattern correlator having different error resistance values in a delimiter. (d) Effect of MPN.

is increased, there is an improvement in the PLR. After 32 preamble bits, we observed error-free operation (PLR $< 10^{-6}$) for any phase step. However, the use of the preamble reduces the effective throughput and increases delay. Also, a 32-bit preamble does not satisfy the 28-bit requirement specified in the G.984.2 [4]. With the introduction of a 20-km of fiber uplink, it can be observed from Fig. 4(a), that there is a degradation in the PLR performance. However, by switching on the burst-mode functionality of the receiver with the CPA, we observe error-free operation in both configurations for any phase step $|\Delta\varphi| \leq 2\pi$ rads with *no* preamble bits, allowing for instantaneous phase acquisition[2]. This is well below the 28-bit GPON specification.

A delimiter of a packet that cannot be detected correctly will lead to the packet being lost. The error resistance of the delimiter depends not only on its length, but also on the exact implementation of the pattern correlator. If the pattern correlator has an error resistance of z bits in a d-bit delimiter, then the PLR at a given BER of p_e can be estimated as

$$\text{PLR} \leq \sum_{j=z+1}^{d} \binom{d}{j} p_e^j (1-p_e)^{d-j} \qquad (8)$$

In Fig. 4(b), we compare experimentally and theoretically, the PLR performance of the GPON uplink as a function of the received power. Our experimental results and the theoretical predictions are in very close agreement. The complexity of the pattern correlator depends on what an acceptable error resistance of the delimiter should be. To get a reasonable indication, consider the plot in Fig. 4(c). This plot shows the PLR performance as a function of the BER for various error resistance values of the delimiter. It can be seen that even with a simple pattern correlator having a 1-bit or a 2-bit error resistance, we obtain PLR $< 10^{-9}$ and PLR $< 10^{-17}$ at a BER $= 10^{-10}$, respectively, which is sufficient for GPONs. In Fig. 4(d), we plot the PLR for various values of the mean square variance of MPN σ_{mpn}. As expected, the system performance degrades with an increase in σ_{mpn}. Recall that the maximum MPN that can be tolerated in the uplink giving an effective coding gain of zero, is when $\sigma_{mpn} \sim 0.14$. At this value of MPN, we obtain a power penalty of 2 dB at a PLR $= 10^{-6}$. There is also a deterioration of more than two orders of magnitude in the PLR for signal power ≥ -13 dBm.

[2]Note, the curves are symmetrical about 0 rads from $-2\pi \leq \Delta\varphi \leq 0$ rads.

IV. Summary and Conclusion

We experimentally demonstrated the performance analysis of a BMRx in a 622 Mb/s 20-km GPON uplink by studying the effect of MPN, and quantified the results in terms of the BER and PLR performance of the system. Our receiver features a CPA for automatic phase acquisition, and an RS$(255, 239)$ decoder for FEC. The BMRx accomplishes a 3 dB coding gain at BER $= 10^{-10}$. The coding gain can be used to reduce the minimum and maximum transmitter power, or increase the minimum receiver sensitivity by the same amount. Alternatively, the effective coding gain can be used to reduce the penalty due to MPN, and thus achieve a longer physical reach or support more splits per single PON tree.

This BMRx provides instantaneous (0 preamble bit) phase acquisition and PLR $< 10^{-6}$ for any phase step ($\pm 2\pi$ rads) between consecutive packets, clearly meeting the 28-bit GPON specification. We note that a sensitivity penalty results from the quick extraction of the decision threshold and clock phase from a short preamble at the start of each packet [12]. However, by reducing the length of the CPA field, as demonstrated in this work, more bits are left for amplitude recovery, thus reducing the burst-mode sensitivity penalty. Alternatively, with the reduced number of preamble bits, more bits can be left for the payload, thereby increasing the information rate.

The price to pay to obtain instantaneous phase acquisition is faster electronics. On the other hand, our solution leverages the design of components for long-haul, transport networks which are typically a generation ahead of the components for multiaccess networks.

References

[1] C.-H. Lee, et. al., *IEEE J. Lightw. Technol.*, vol. 24, no. 12, 2006.
[2] T. Koonen, *IEEE Proceedings*, vol.94, no.5, 2006.
[3] G. P. Agarwal, *Fiber-Optic Communication Systems*, 3rd ed. New York: Wiley, 2002.
[4] *Gigabit-capable Passive Optical Networks: Physical Media Dependent layer specification*, ITU-T Recommendation G.984.2., 2003.
[5] J. Faucher, et. al., in *Proc. IEEE Laser and Electro-Optics*, Paper TuDD3, 2006.
[6] B. J. Shastri, et. al., in *Proc. IEEE Midwest Symposium on Circuits and Systems*, pp. 120-123, 2007.
[7] J. W. Goodman, *Statistical Optics*, New York: Wiley, 2000.
[8] B. Sklar, *Digital Communications: Fundamentals and Applications*, 2nd ed. Upper Saddle River: Prentice Hall, 2001.
[9] K. Ogawa, *IEEE J. Quantum Electron.*, vol. 18, no. 5, 1982.
[10] G. P. Agrawal, et. al., *IEEE J. Lightw. Technol.*, vol. 6, no. 5, 1988.
[11] X. Liu, et. al., in *Proc. Optical Fiber Communication Conf.*, vol. 1, 2005.
[12] P. Ossieur, et. al., *IEEE J. Lightw. Technol.*, vol. 21, no. 11, 2003.